

## Corroles with Group 15 Ions. 2. Synthesis and Characterization of Octaethylcorroles Containing a Phosphorus Central Atom

Karl M. Kadish,<sup>\*,†</sup> Zhongping Ou,<sup>†</sup> Victor A. Adamian,<sup>†,‡</sup> Roger Guilard,<sup>§</sup> Claude P. Gros,<sup>§</sup> Christoph Erben,<sup>||,⊥</sup> Stefan Will,<sup>||</sup> and Emanuel Vogel<sup>\*,||</sup>

Department of Chemistry, University of Houston, Houston, Texas 77204-5641, Université de Bourgogne, LIMSAG UMR 5633, Faculté des Sciences Gabriel, 6, Boulevard Gabriel, 21000 Dijon, France, and Institut für Organische Chemie, Universität zu Köln, Greinstrasse 4, 50939 Köln, Germany

Received August 25, 2000

The synthesis, spectroscopic characterization, and electrochemistry of five new phosphorus corroles are reported. The investigated complexes contain alkyl, aryl, oxo, or hydrido axial ligands and are represented as (OEC)P(H)<sub>2</sub>, (OEC)P(CH<sub>3</sub>)<sub>2</sub>, (OEC)P(C<sub>6</sub>H<sub>5</sub>)<sub>2</sub>, (OEC)P=O, and [(OEC)P(CH<sub>3</sub>)<sub>2</sub>]<sup>+</sup>ClO<sub>4</sub><sup>-</sup>, where OEC is the trianion of octaethylcorrole. The products of electrooxidation and/or electroreduction were also characterized by UV–vis and ESR spectroscopy. Correlations are shown to exist between reversible half-wave potentials for the first oxidation and first reduction of each compound and the combined electronegativity of the central ion and the axial ligand(s). The electrochemical HOMO–LUMO gap, defined as the difference between first reduction and first oxidation, was found to be independent of the electron-transfer site and similar in magnitude to the value generally observed for metalloporphyrins with planar macrocycles, i.e., 2.25 ± 0.15 V.

### Introduction

Numerous studies have recently been devoted to metallo-corroles<sup>1–19</sup> whose coordination and electrochemical properties have often been compared to the analogous metalloporphyrins. The corrole macrocycle has a direct pyrrole–pyrrole bond but retains nevertheless an 18  $\pi$ -electron aromatic system and properties generally associated with porphyrins. The contracted ring has a –3 charge for the macrocycle in its deprotonated form and often leads to a stabilization of metal ions in an oxidation state higher than in the case of metalloporphyrins where the deprotonated free base macrocycle has a charge of –2. For example, air-stable Fe(IV) complexes of [(OEC)Fe]<sub>2</sub>O

and (OEC)Fe(C<sub>6</sub>H<sub>5</sub>), where OEC = 2,3,7,8,12,13,17,18-octaethylcorrole, are known and both compounds can be oxidized to give formally Fe(V) corrole  $\pi$ -cation radicals and/or dications.<sup>6,9</sup> (OEC)FeCl has also been characterized as containing an Fe(IV) center,<sup>6,9</sup> but recent results suggest the possibility that this compound might also exist as an Fe(III)  $\pi$ -cation radical.<sup>12</sup>

In theory, a large number of metal ions can be inserted into the corrole cavity but the coordination chemistry of this macrocycle has been limited in large part to first-row transition metals.<sup>1,2</sup> There are only a few examples in the literature of metallo-corroles containing main group elements,<sup>1,2,16–19</sup> while the “periodic table of metalloporphyrins” has been extensively studied, even with the same group 15 elements.<sup>20–33</sup>

<sup>†</sup> University of Houston.

<sup>‡</sup> Current address: BP, 150 West Warrenville Road, Naperville, IL 60563.

<sup>§</sup> Université de Bourgogne.

<sup>||</sup> Universität zu Köln.

<sup>⊥</sup> Current address: Lucent Technologies—Bell Laboratories, Murray Hill, New Jersey 07974.

- (1) Erben, C.; Will, S.; Kadish, K. M. In *The Porphyrin Handbook*; Kadish, K. M., Smith, K. M., Guilard, R., Eds.; Academic Press: Burlington, MA, 2000; Vol. 2, pp 233–300.
- (2) Paolesse, R. In *The Porphyrin Handbook*; Kadish, K. M., Smith, K. M., Guilard, R., Eds.; Academic Press: Burlington, MA, 2000; Vol. 2, pp 201–232.
- (3) (a) Genokhova, N. S.; Melent'eva, T. A.; Berezovskii, V. M. *Russ. Chem. Rev.* **1980**, *49*, 1056. (b) Melent'eva, T. A. *Russ. Chem. Rev.* **1983**, *52*, 641.
- (4) Licoccia, S.; Paolesse, R. *Struct. Bonding* **1995**, *84*, 71.
- (5) Autret, M.; Will, S.; Van Caemelbecke, E.; Lex, J.; Gisselbrecht, J.-P.; Gross, M.; Vogel, E.; Kadish, K. M. *J. Am. Chem. Soc.* **1994**, *116*, 9141.
- (6) Van Caemelbecke, E.; Will, S.; Autret, M.; Adamian, V. A.; Lex, J.; Gisselbrecht, J.-P.; Gross, M.; Vogel, E.; Kadish, K. M. *Inorg. Chem.* **1996**, *35*, 184.
- (7) Will, S.; Lex, J.; Vogel, E.; Adamian, V. A.; Van Caemelbecke, E.; Kadish, K. M. *Inorg. Chem.* **1996**, *35*, 5577.
- (8) Will, S.; Lex, J.; Vogel, E.; Schmickler, H.; Gisselbrecht, J.-P.; Hauptmann, C.; Bernard, M.; Gross, M. *Angew. Chem., Int. Ed. Engl.* **1997**, *36*, 357; *Angew. Chem.* **1997**, *109*, 367.

- (9) Vogel, E.; Will, S.; Schulze Tilling, A.; Neumann, L.; Lex, J.; Bill, E.; Trautwein, A. X.; Wieghardt, K. *Angew. Chem., Int. Ed. Engl.* **1994**, *33*, 731; *Angew. Chem.* **1994**, *106*, 771.
- (10) Licoccia, S.; Morgante, E.; Paolesse, R.; Polizio, F.; Senge, M. O.; Tondello, E.; Boschi, T. *Inorg. Chem.* **1997**, *36*, 1564.
- (11) Kadish, K. M.; Adamian, V. A.; Van Caemelbecke, E.; Gueletii, E.; Will, S.; Erben, C.; Vogel, E. *J. Am. Chem. Soc.* **1998**, *120*, 11986.
- (12) Cai, S.; Walker, F. A.; Licoccia, S. *Inorg. Chem.* **2000**, *39*, 3466.
- (13) Meier-Callahan, A. E.; Gray, H. B.; Gross, Z. *Inorg. Chem.* **2000**, *39*, 3605.
- (14) Gross, Z.; Simkhovich, L.; Galili, N. *J. Chem. Soc., Chem. Commun.* **1999**, 599.
- (15) Simkhovich, L.; Galili, N.; Saltsman, I.; Goldberg, I.; Gross, Z. *Inorg. Chem.* **2000**, *39*, 2704.
- (16) Kadish, K. M.; Will, S.; Adamian, V. A.; Walther, B.; Erben, C.; Ou, Z.; Guo, N.; Vogel, E. *Inorg. Chem.* **1998**, *37*, 4573.
- (17) Paolesse, R.; Licoccia, S.; Boschi, T. *Inorg. Chim. Acta* **1990**, *178*, 9.
- (18) Paolesse, R.; Boschi, T.; Licoccia, S.; Khoury, R. G.; Smith, K. M. *J. Chem. Soc., Chem. Commun.* **1998**, 1119.
- (19) Kadish, K. M.; Erben, C.; Ou, Z.; Adamian, V. A.; Will, S.; Vogel, E. *Inorg. Chem.* **2000**, *39*, 3312.
- (20) Treibs, A. *Liebigs Ann. Chem.* **1969**, *728*, 115.
- (21) Sayer, P.; Gouterman, M.; Connell, C. R. *Acc. Chem. Res.* **1982**, *15*, 73.
- (22) Sayer, P.; Gouterman, M.; Connell, C. R. *J. Am. Chem. Soc.* **1977**, *99*, 1082.
- (23) Knör, G.; Vogler, A. *Inorg. Chem.* **1994**, *33*, 314.

It was recently shown that (EMC)H<sub>3</sub>, where EMC = 8,12-diethyl-2,3,7,13,17,18-hexamethylcorrole, reacts with POCl<sub>3</sub> in pyridine to give (EMC)P<sup>V</sup>(OH)Cl, as confirmed by an X-ray characterization of this complex.<sup>18</sup> In this paper, we report the synthesis, spectroscopic characterization, and electrochemistry of phosphorus octaethylcorroles with a variety of different types of axial ligands, none of which have previously been characterized. The investigated P(V) complexes contain alkyl, aryl, oxo, or hydrido axial ligands and are represented as (OEC)P=O, (OEC)P(H)<sub>2</sub>, (OEC)P(CH<sub>3</sub>)<sub>2</sub>, (OEC)P(C<sub>6</sub>H<sub>5</sub>)<sub>2</sub>, and [(OEC)P(CH<sub>3</sub>)]<sup>+</sup>ClO<sub>4</sub><sup>-</sup>. The electrochemistry of each corrole is elucidated in PhCN, 0.1 M TBAP, and the products of electrooxidation and/or electroreduction are characterized by UV-vis and ESR spectroscopy.

In a preceding paper, we reported the synthesis and electrochemistry of octaethylcorroles containing As, Sb, and Bi, each of which could exist in three different oxidation states.<sup>19</sup> The electrochemical data for these group 15 derivatives are combined in the present paper with that of the five new phosphorus complexes as well as with data for the oxidation and reduction of other corroles containing different central ions in order to obtain a self-consistent picture of how the overall electron density at the central metal affects the corrole redox potentials and HOMO-LUMO gap. Comparisons are also made between octaethylcorroles and octaethylporphyrins containing the same central ions.

## Experimental Section

**Instrumentation.** <sup>1</sup>H, <sup>13</sup>C NMR, and <sup>31</sup>P NMR spectra were recorded at 300 MHz/75.5 MHz/121.5 MHz on a Bruker AP 300 NMR spectrometer. The CDCl<sub>3</sub> solvent signals were used as a standard at δ = 7.24 (<sup>1</sup>H) and δ = 77.0 (<sup>13</sup>C), while H<sub>3</sub>PO<sub>4</sub> was used as an external standard for <sup>31</sup>P measurements. UV-visible spectra were recorded on a Perkin-Elmer Lambda 7 spectrophotometer, while IR measurements were performed with a Perkin-Elmer IR spectrophotometer 283 or a Perkin-Elmer series 1600. ESR spectra were recorded on an IBM ER 100D or on a Bruker ESP 380E spectrometer. The *g* values were measured with respect to diphenylpicrylhydrazyl (*g* = 2.0036 ± 0.0003). Electron ionization mass spectra were taken on a Finnigan 3200 or Finnigan MAT 212 instrument. FAB spectra were recorded on a Varian MAT 731 mass spectrometer. Elemental analysis was provided by Bayer AG, Leverkusen, Germany.

Cyclic voltammetry was carried out with an EG&G model 173 potentiostat or an IBM model EC 225 voltammetric analyzer. A three-electrode system was used and consisted of a glassy carbon or platinum disk working electrode, a platinum wire counter electrode, and a saturated calomel electrode (SCE) as the reference electrode. The SCE was separated from the bulk of the solution by a fritted-glass bridge of low porosity, which contained the solvent/supporting electrolyte mixture. All potentials are referenced to the SCE. UV-visible

spectroelectrochemical experiments were carried out with a Hewlett-Packard model 8453 diode array spectrophotometer.

**Chemicals.** Benzonitrile (PhCN) was purchased from Aldrich Chemical Co. and distilled over P<sub>2</sub>O<sub>5</sub> under vacuum prior to use. Absolute dichloromethane (CH<sub>2</sub>Cl<sub>2</sub>) was purchased from Aldrich Chemical Co. and used without further purification. CDCl<sub>3</sub> for NMR measurements was obtained from Aldrich Chemical Co. and used as received. Tetra-*n*-butylammonium perchlorate was purchased from Sigma Chemical Co., recrystallized from ethyl alcohol, and dried under vacuum at 40 °C for at least 1 week prior to use. The investigated compounds were synthesized as described below.

**1. (OEC)P=O.** A total of 1.0 mL of phosphorus trichloride was added to a solution of 523 mg (1 mmol) of octaethylcorrole in 20 mL of pyridine with stirring. After 5 min the volatile compounds were removed in vacuo. A total of 50 mL of water was added, and the mixture was further stirred for 30 min. The red precipitate was collected and washed thoroughly with water. The phosphorus compound was obtained after passing through a short column of alumina (Brockmann) using dichloromethane as eluent. The red band contained the title compound, which was obtained as red powder after crystallization from hexane (460 mg, 81%). <sup>1</sup>H NMR (300 MHz, CDCl<sub>3</sub>): δ 9.79 (singlet, 2H, H-5,15), 9.61 (singlet, 1H, H-10), 4.07–3.88 (multiplets, 16H, CH<sub>2</sub>), 1.79 (triplet, 6H, CH<sub>3</sub>), 1.78 (triplet, 6H, CH<sub>3</sub>), 1.76 (triplet, 6H, CH<sub>3</sub>), 1.75 (triplet, 6H, CH<sub>3</sub>). <sup>13</sup>C NMR (75.5 MHz, CDCl<sub>3</sub>): δ 138.90, 138.60, 137.38, 137.22, 133.44, 133.33, 129.00, 124.64, 93.19 (C-10), 90.74 (C-5,15), 20.34, 20.01, 19.84, 19.58, 18.30, 18.20, 17.51, 17.61. <sup>31</sup>P NMR (121.5 MHz, CDCl<sub>3</sub>/H<sub>3</sub>PO<sub>4</sub> ext): δ -99.40. MS (EI, 70 eV): *m/z* (%) 566 (100) M<sup>+</sup>, 551 (14) [M - CH<sub>3</sub>]<sup>+</sup>, 536 (6) [M - 2CH<sub>3</sub>]<sup>+</sup>, 283 (15) [M]<sup>2+</sup>, 268 (11) [M - CH<sub>3</sub>]<sup>2+</sup>. IR (CsI), *ν*: 2966, 2932, 2870, 1530, 1466, 1449, 1286, 1186, 1158, 1056, 1028, 1014, 960, 900, 812 cm<sup>-1</sup>. UV-vis (CH<sub>2</sub>Cl<sub>2</sub>), λ<sub>max</sub> (nm) (ε × 10<sup>-4</sup>, mol<sup>-1</sup> L cm<sup>-1</sup>): 273 (0.4), 315 (0.4), 402 (12.5), 520 (0.5), 561 (1.6). Anal. Calcd for C<sub>73</sub>H<sub>43</sub>N<sub>4</sub>PO: C, 74.18; H, 7.65; N, 9.89. Found: C, 73.90; H, 7.33; N, 10.17.

**2. (OEC)P(H)<sub>2</sub>.** A suspension of 567 mg (1 mmol) of (OEC)P=O and 380 mg (10 mmol) of LiAlH<sub>4</sub> in 50 mL of diethyl ether was refluxed for 30 min under an argon atmosphere. During this time the color changed from red to green-blue. The mixture was then hydrolyzed by adding methanol and water at -30 °C, and the filtered solution was evaporized to dryness in vacuo. The residue was passed through a short column of alumina under argon atmosphere (Brockmann) using dichloromethane as eluent. The first band contained the dihydrido complex, which was obtained after crystallization from dichloromethane/methanol as violet needles (yield: 332 mg, 60%). <sup>1</sup>H NMR (300 MHz, CDCl<sub>3</sub>): δ 9.61 (singlet, 2H, H-5,15), 9.38 (singlet, 1H, H-10), 4.07 (quartet, 4H, CH<sub>2</sub>), 4.06 (quartet, 4H, CH<sub>2</sub>), 4.04 (quartet, 8H, CH<sub>2</sub>), 1.93 (triplet, 6H, CH<sub>3</sub>), 1.90 (triplet, 6H, CH<sub>3</sub>), 1.89 (triplet, 12H, CH<sub>3</sub>), -3.31 (doublet, <sup>1</sup>J<sub>PH</sub> = 921 Hz, 2H, P-H). <sup>13</sup>C NMR (75.5 MHz, CDCl<sub>3</sub>): δ 137.97, 136.93, 136.89, 134.43, 134.28, 128.31, 127.76, 127.68, 89.52, 83.72, 20.56, 19.83, 19.78, 19.63, 18.88, 18.85, 18.31, 18.19. <sup>31</sup>P NMR (121.5 MHz, CDCl<sub>3</sub>): δ -252.52 (triplet, <sup>1</sup>J<sub>PH</sub> = 916 Hz). MS (EI, 70 eV): *m/z* (%) 552 (97) M<sup>+</sup>, 551 (100) [M - H]<sup>+</sup>, 550 (11) [M - 2H]<sup>+</sup>, 537 (7) [M - CH<sub>3</sub>]<sup>+</sup>, 522 (9) [M - 2CH<sub>3</sub>]<sup>+</sup>, 276 (15) [M]<sup>2+</sup>. IR (CsI), *ν*: 2964, 2930, 2868, 2281 (*ν*<sub>PH</sub>), 1501, 1480, 1466, 1394, 1372, 1280, 1206, 1170, 959, 890, 804, 789, 758 cm<sup>-1</sup>. UV-vis (CH<sub>2</sub>Cl<sub>2</sub>), λ<sub>max</sub>(nm) (ε × 10<sup>-4</sup>, mol<sup>-1</sup> L cm<sup>-1</sup>): 317 (3.3), 429 (17.2), 444 (22.5), 553 (1.1), 595 (1.4), 634 (3.0).

**3. [(OEC)P(CH<sub>3</sub>)]<sup>+</sup>ClO<sub>4</sub><sup>-</sup>.** Methylmagnesium iodide was added dropwise to a solution of 567 mg (1 mmol) of (OEC)P=O in 25 mL of dichloromethane until no starting compound could be detected by thin-layer chromatography (silica gel/dichloromethane; starting compound pink spot with *R<sub>f</sub>* of 0, monomethyl compound purple spot with *R<sub>f</sub>* of 0.5). The purple solution was washed with aqueous ammonium chloride, and the volatile compounds were removed in vacuo. The residue was then chromatographed on silica gel using dichloromethane as eluent. The eluate of the second (purple) band was collected and concentrated to a volume of 5 mL, after which 5 mL of methanol and 0.2 mL of perchloric acid were added and the dichloromethane removed by gentle heating in a water bath. The title compound was obtained after crystallization at -20 °C as red parallelograms that were washed thoroughly with water and dried in vacuo (yield: 452 mg, 68%).

- (24) Liu, Y. H.; Bénassy, M.-F.; Chojnacki, S.; D'Souza, F.; Barbour, T.; Belcher, W. J.; Brothers, P. J.; Kadish, K. M. *Inorg. Chem.* **1994**, *33*, 4480.
- (25) Akiba, K.-y.; Onzuka, Y.; Itagaki, M.; Hirota, H.; Yamamoto, Y. *Organometallics* **1994**, *13*, 2800.
- (26) Satoh, W.; Nadano, R.; Yamamoto, G.; Yamamoto, Y.; Akiba, K.-y. *Organometallics* **1997**, *16*, 3664.
- (27) Yamamoto, Y.; Nadano, R.; Itagaki, M.; Akiba, K.-y. *J. Am. Chem. Soc.* **1995**, *117*, 8287.
- (28) Kadish, K. M.; Autret, M.; Ou, Z.; Akiba, K.-y.; Masumoto, S.; Wada, R.; Yamamoto, Y. *Inorg. Chem.* **1996**, *35*, 5564.
- (29) Marrese, C. A.; Carrano, C. J. *Inorg. Chem.* **1984**, *23*, 3961.
- (30) Vangberg, T.; Ghosh, A. *J. Am. Chem. Soc.* **1999**, *121*, 12154.
- (31) Segewa, H.; Kunitomo, K.; Nakamoto, A.; Shimidzu, T. *J. Chem. Soc., Perkin Trans. 1* **1992**, 939.
- (32) Michaudet, L.; Fasseur, D.; Guillard, R.; Ou, Z.; Kadish, K. M.; Dahanoui, S.; Lecomte, C. *J. Porphyrins Phthalocyanines* **2000**, *4*, 261.
- (33) *The Porphyrin Handbook*; Kadish, K. M., Smith, K. M., Guillard, R., Eds.; Academic Press: Burlington, MA, 2000; Vols. 1–10.

**Caution!** Organic perchlorate salts can detonate spontaneously. Although no explosions were encountered in this work, precautions are warranted. The preparation of [(OEC)P(CH<sub>3</sub>)<sup>+</sup>ClO<sub>4</sub><sup>-</sup>] was always done on a small scale, and the material was not stored for long periods. <sup>1</sup>H NMR (300 MHz, CDCl<sub>3</sub>): δ 10.19 (singlet, 2H, H-5,15), 10.10 (singlet, 1H, H-10), 4.33–4.04 (multiplets, 16 H, CH<sub>2</sub>), 1.94 (quartet, 6H, CH<sub>3</sub>), 1.90 (quartet, 6H, CH<sub>3</sub>), 1.87 (quartet, 12H, CH<sub>3</sub>), -4.50 (doublet, <sup>2</sup>J<sub>PH</sub> = 16.0 Hz, 6H, P-CH<sub>3</sub>). <sup>13</sup>C NMR (75.5 MHz, CDCl<sub>3</sub>): δ 142.68, 139.65, 138.00, 136.47, 136.42, 133.45, 132.39, 125.59, 94.65 (C-10), 92.31 (C-5,15), 20.52, 20.16, 20.01, 19.68, 18.07, 18.04, 17.46, 17.42, 16.69 (doublet, <sup>1</sup>J<sub>PC</sub> = 152.9 Hz, P-CH<sub>3</sub>). <sup>31</sup>P NMR (121.5 MHz, CDCl<sub>3</sub>/H<sub>3</sub>PO<sub>4</sub> ext): δ -94.32 (quartet, <sup>2</sup>J<sub>PH</sub> = 16 Hz). MS (FAB/NBA): *m/z* (%) 565 (100) [(OEC)P(CH<sub>3</sub>)<sup>+</sup>]. IR (CsI), *ν*: 2967, 2933, 2873, 1465, 1094, 1057, 1019, 966, 624 cm<sup>-1</sup>. UV-vis (CH<sub>2</sub>Cl<sub>2</sub>), λ<sub>max</sub>(nm) (ε × 10<sup>-4</sup>, mol<sup>-1</sup> L cm<sup>-1</sup>) = 281 (1.9), 390 (3.9) sh, 410 (22.6), 502 (0.4) sh, 528 (1.7), 568 (2.4). Anal. Calcd for C<sub>36</sub>H<sub>46</sub>N<sub>4</sub>PClO<sub>4</sub>: C, 65.00; H, 6.97; N, 8.42. Found: C, 65.89; H, 6.93; N, 8.68.

**4. (OEC)P(CH<sub>3</sub>)<sub>2</sub>.** Methylmagnesium iodide (4 mmol) in diethyl ether was added to a solution of 665 mg (1 mmol) of [(OEC)P(CH<sub>3</sub>)<sup>+</sup>ClO<sub>4</sub><sup>-</sup>] in 20 mL of dichloromethane. After hydrolysis, the volatile compounds were removed in vacuo. The title compound was obtained after passing the residue through a short column of alumina (Brockmann) using dichloromethane. The purple band contained the title compound, which was obtained after crystallization from dichloromethane/methanol as violet needles with metallic luster (yield: 451 mg, 78%). <sup>1</sup>H NMR (300 MHz, CDCl<sub>3</sub>): δ 9.60 (singlet, 2 H, H-5,15), 9.42 (singlet, 1H, H-10), 4.21 (quartet, 4H, CH<sub>2</sub>), 4.13 (quartet, 4H, CH<sub>2</sub>), 4.09 (quartet, 8H, CH<sub>2</sub>), 1.98 (triplet, 6H, CH<sub>3</sub>), 1.95 (triplet, 6H, CH<sub>3</sub>), 1.94 (triplet, 12H, CH<sub>3</sub>), -6.23 (doublet, 6H, <sup>2</sup>J<sub>PH</sub> = 17.4 Hz, P-CH<sub>3</sub>). <sup>13</sup>C NMR (75.5 MHz, CDCl<sub>3</sub>): δ 136.88, 135.98, 135.84, 133.94, 132.63, 127.73, 127.15, 125.18, 88.97 (C-5,15), 83.80 (C-10), 34.13 (doublet, <sup>1</sup>J<sub>PC</sub> = 230 Hz), 20.61, 19.86, 19.77, 19.69, 18.94, 18.92, 18.39, 18.27. MS (EI, 70 eV): *m/z* (%) 580 (8) M<sup>+</sup>, 565 (100) [M - CH<sub>3</sub>]<sup>+</sup>, 550 (9) [M - 2CH<sub>3</sub>]<sup>+</sup>, 283 (14) [M - CH<sub>3</sub>]<sup>2+</sup>. UV-vis (CH<sub>2</sub>-Cl<sub>2</sub>), λ<sub>max</sub>(nm) (ε × 10<sup>-4</sup>, mol<sup>-1</sup> L cm<sup>-1</sup>): 316 (2.4), 412 (4.3), 423 (17.3), 435 (22.2), 543 (1.1), 570 (1.0), 586 (1.9), 617 (3.2). Anal. Calcd for C<sub>37</sub>H<sub>49</sub>N<sub>4</sub>P: C, 76.52; H, 8.50; N, 9.65. Found: C, 76.48; H, 8.41; N, 10.01.

**5. (OEC)P(C<sub>6</sub>H<sub>5</sub>)<sub>2</sub>.** A solution of 567 mg (1 mmol) of (OEC)P=O in 10 mL of dichloromethane containing 2 mL of methanol was stirred for 30 min to generate a reactive dimethoxy derivative. The volatile compounds were removed in vacuo, after which 10 mL of dichloromethane and 4 mmol of phenylmagnesium bromide in diethyl ether were added. After 10 min the mixture was hydrolyzed and the organic layer washed with water and evaporated to dryness. The residue was passed through a short column of alumina (Brockmann) using dichloromethane as eluent. (OEC)P(C<sub>6</sub>H<sub>5</sub>)<sub>2</sub> was obtained after crystallization from hexane as purple cubes with a yield of 444 mg (63%). <sup>1</sup>H NMR (300 MHz, CDCl<sub>3</sub>): δ 9.46 (singlet, 2H, H-5,15), 9.24 (singlet, 1H, H-10), 5.33 (multiplet, 1H, phenyl *p*-H), 4.85 (multiplet, 2 H, phenyl, *m*-H) 4.10 (quartet, 4H, CH<sub>2</sub>), 4.02 (quartet, 4H, CH<sub>2</sub>), 4.00 (quartet, 4H, CH<sub>2</sub>), 3.98 (quartet, 4H, CH<sub>2</sub>), 1.90 (triplet, 6H, CH<sub>3</sub>), 1.84 (triplet, 6H, CH<sub>3</sub>), 1.83 (triplet, 6H, CH<sub>3</sub>), 1.81 (triplet, 6H, CH<sub>3</sub>), 0.39 (multiplet, 2H, phenyl *o*-H). <sup>13</sup>C NMR (75.5 MHz, CDCl<sub>3</sub>): δ = 154.33 (doublet, <sup>1</sup>J<sub>CP</sub> = 265 Hz, phenyl, C<sub>ipso</sub>) 138.44, 137.20, 136.94, 134.86, 134.72, 128.59, 128.37, 127.41, 123.29 (doublet, <sup>1</sup>J<sub>CP</sub> = 22.4 Hz, phenyl), 122.85 (doublet, <sup>1</sup>J<sub>CP</sub> = 16.5 Hz, phenyl), 122.42 (doublet, <sup>1</sup>J<sub>CP</sub> = 4.7 Hz, phenyl *p*-C), 89.77 (C-5,15), 84.80 (C-10), 20.61, 19.89, 19.78, 19.61, 18.84, 18.65, 18.26, 18.15. <sup>31</sup>P NMR (121.5 MHz, CDCl<sub>3</sub>/H<sub>3</sub>PO<sub>4</sub> ext): δ -215.94 (multiplet). IR (CsI), *ν*: 3059, 2966, 2930, 2870, 1501, 1464, 1448, 1430, 1391, 1376, 1281, 1194, 1162, 1087, 1057, 1030, 1017, 964, 893, 796, 749, 716, 690, 540 cm<sup>-1</sup>. UV-vis (CH<sub>2</sub>Cl<sub>2</sub>), λ<sub>max</sub>(nm) (ε × 10<sup>-4</sup>, mol<sup>-1</sup> L cm<sup>-1</sup>): 314 (2.8), 411 (3.0), 429 (18.7), 440 (23.8), 543 (1.1), 586 (2.2), 616 (3.3).

## Results and Discussion

**Synthesis of (OEC)P=O.** Phosphorus can be incorporated into the octaethylcorrole macrocycle by reaction of the free base corrole ligand with phosphorus(III) chloride in a basic solvent followed by conventional workup. This reaction gives (OEC)P=O

**Table 1.** Selected <sup>1</sup>H NMR δ Values of Phosphorus Octaethylcorroles

compound	axial ligand	macrocycle			
		H-5,15	H-10	CH <sub>2</sub>	CH <sub>3</sub>
(OEC)P=O		9.79	9.61	4.07–3.88	1.79–1.75
(OEC)P(H) <sub>2</sub>	-3.31	9.61	9.38	4.07–4.04	1.93–1.89
(OEC)P(CH <sub>3</sub> ) <sub>2</sub>	-6.23	9.60	9.42	4.21–4.09	1.98–1.94
(OEC)P(C <sub>6</sub> H <sub>5</sub> ) <sub>2</sub>	5.33, 4.85, 0.39	9.46	9.24	4.10–3.98	1.90–1.81
[(OEC)P(CH <sub>3</sub> ) <sup>+</sup> ClO <sub>4</sub> <sup>-</sup> ]	-4.50	10.19	10.10	4.33–4.04	1.94–1.87

in high yields, and a hydroxy corrole derivative that was reported with a similar reaction procedure using a different corrole<sup>18</sup> could not be detected. The formation of an oxophosphorus(V) corrole is quite different from what is observed for other group 15 corroles that form four-coordinate (OEC)M<sup>III</sup> derivatives where M = As, Sb, or Bi.<sup>19</sup> As indicated above, no evidence for [(OEC)P(OH)]<sup>+</sup> was seen nor was any P(III) product detected during the metalation reaction.

The <sup>1</sup>H NMR spectrum of (OEC)P=O shows characteristic features of a diamagnetic aromatic compound. Resonances of the meso protons H-5,15 and H-10 are located at δ 9.79 and 9.61 (Table 1), confirming a strong diamagnetic ring current effect. Protons of the CH<sub>2</sub> units give rise to multiplets (AB part of a ABX<sub>3</sub> spin system) around 4 ppm. This diastereotopism indicates the lack of a horizontal symmetry plane and leads to the conclusion that the central phosphorus ion adopts an out-of-plane position with one axial ligand.

**Synthesis of [(OEC)P<sup>V</sup>(CH<sub>3</sub>)<sup>+</sup>ClO<sub>4</sub><sup>-</sup>].** The formation of a monomethyl corrole derivative was achieved by reaction of (OEC)P=O with methylmagnesium iodide. The perchlorate salt was obtained by treatment of the above reaction product with perchloric acid. Formulation of the product as a compound that is methylated at the central ion is based on its NMR spectrum, which indicates the presence of an aromatic compound with C<sub>s</sub> symmetry. The meso-proton resonances of [(OEC)P(CH<sub>3</sub>)<sup>+</sup>ClO<sub>4</sub><sup>-</sup>] appear as two singlets at δ = 10.19 and 10.10, while the CH<sub>2</sub> units of the ethyl groups correspond to multiplets at δ = 4.33–4.04. The resonance of the methyl group bound to the central ion occurs at high field. A doublet centered at δ -4.50 with a <sup>1</sup>H–<sup>31</sup>P coupling constant of 16.0 Hz is observed (Table 1). The strong shielding seen for the methyl protons is a result of the magnetic anisotropy of the aromatic corrole macrocycle. The resonances of the corrole protons in the monomethyl compounds are shifted to lower field compared to the neutral (OEC)P=O, and this is due to the presence of a positive charge on [(OEC)P<sup>V</sup>(CH<sub>3</sub>)<sup>+</sup>ClO<sub>4</sub><sup>-</sup>].

**Synthesis of (OEC)P(L)<sub>2</sub>, Where L = H, *σ*-Methyl or *σ*-Phenyl.** The synthesis of these phosphorus derivatives are shown in Scheme 1. The dihydrido compound, (OEC)P(H)<sub>2</sub>, was obtained as an actual reaction product during attempts to reduce (OEC)P=O to (OEC)P using lithium aluminum hydride.

The reaction of (OEC)P=O with excess Grignard reagent leads to the neutral *σ*-bonded organophosphorus compounds in low to moderate yield. However, (OEC)P(CH<sub>3</sub>)<sub>2</sub> is obtained in distinctly higher yield if the monomethyl compound, [(OEC)P(CH<sub>3</sub>)<sup>+</sup>ClO<sub>4</sub><sup>-</sup>], is reacted with methylmagnesium iodide. In the case of (OEC)P(C<sub>6</sub>H<sub>5</sub>)<sub>2</sub>, it is advantageous to convert (OEC)P=O to the more reactive dimethoxy compound in situ prior to reaction with phenylmagnesium bromide. Attempts to prepare the monophenyl compound, [(OEC)P(C<sub>6</sub>H<sub>5</sub>)<sup>+</sup>], by reaction of (OEC)P=O with stoichiometric amounts of PhMgBr failed, as did a reaction of the free base corrole with PhPCl<sub>2</sub>.

The three (OEC)P(L)<sub>2</sub> compounds with L = H, CH<sub>3</sub>, or C<sub>6</sub>H<sub>5</sub> are stable in the solid state. However, only the *σ*-bonded

## Scheme 1

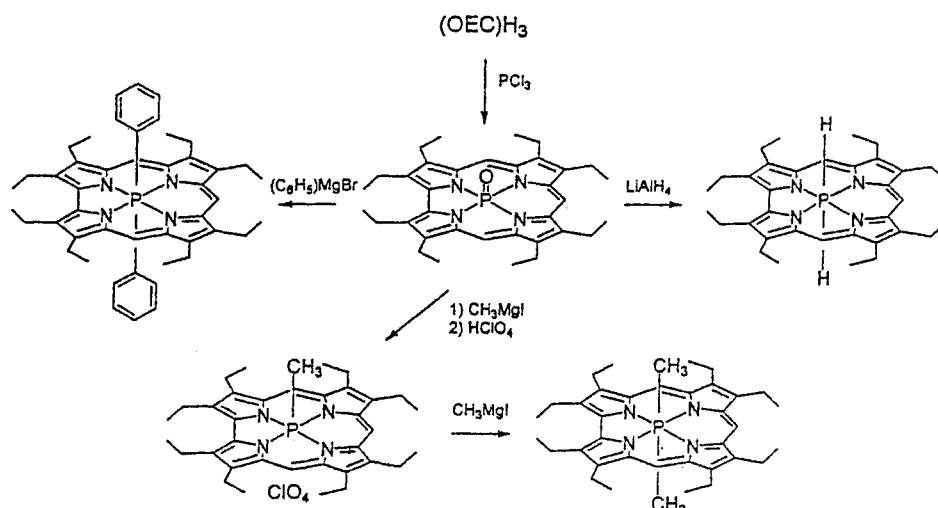


**Table 2.** UV–Visible Spectral Data of (OEC)P=O, (OEC)P(L)<sub>2</sub> (Where L = H, CH<sub>3</sub>, or C<sub>6</sub>H<sub>5</sub>) and [(OEC)P(CH<sub>3</sub>)<sub>2</sub>]<sup>+</sup>ClO<sub>4</sub><sup>−</sup> in a Solution of PhCN and 0.1 M TBAP

compound	$\lambda$ , nm ( $\epsilon \times 10^{-4}$ )					
(OEC)P=O	316 (1.4)	374 <sup>a</sup> (3.5)	404 (24.7)	522 (1.3)	562 (3.5)	
(OEC)P(H) <sub>2</sub>	318 (3.0)	368 (1.8)	432 (13.9)	530 (0.8)	596 (1.3)	634 (2.6)
(OEC)P(CH <sub>3</sub> ) <sub>2</sub>	317 (1.8)	414 <sup>a</sup> (3.1)	425 (13.0)	543 (0.7)	587 (1.4)	618 (2.5)
(OEC)P(C <sub>6</sub> H <sub>5</sub> ) <sub>2</sub>	317 (1.5)	418 <sup>a</sup> (2.3)	431 (13.8)	544 (0.6)	587 (1.5)	617 (2.5)
[(OEC)P(CH <sub>3</sub> ) <sub>2</sub> ] <sup>+</sup>	318 (0.9)	389 <sup>a</sup> (2.6)	412 (17.1)	531 (1.2)	569 (1.6)	

<sup>a</sup> Shoulder.

derivatives are stable in solution and (OEC)P(H)<sub>2</sub> is slowly converted to (OEC)P=O, a process that is strongly enhanced by illumination. The resulting UV–visible spectral changes for this transition are shown in Figure 1.

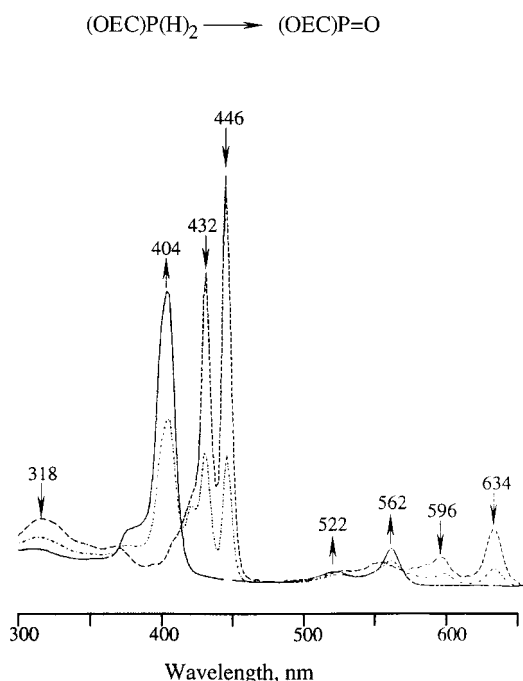


**Figure 1.** UV–visible spectral changes of (OEC)P(H)<sub>2</sub> upon exposure to air and light in a solution of PhCN and 0.1 M TBAP. The final product (shown by a solid line) has absorption bands at 404, 522, and 562 nm and is identified as (OEC)P=O (see Table 2).

The <sup>1</sup>H NMR spectra of (OEC)P(L)<sub>2</sub> are in agreement with the spectra of aromatic compounds of C<sub>2v</sub> symmetry. The <sup>1</sup>H NMR data of these complexes are shown in Table 1. The meso protons H-5,15 and H-10 give singlet signals in the region  $\delta$  9.61–9.24, while the protons of the ethyl groups appear as quartets and triplets. The protons of the axially bound ligands give rise to signals with characteristic phosphorus coupling. For the phosphorus bound hydrogen in (OEC)P(H)<sub>2</sub>, a doublet at  $\delta$  −3.31 with a large <sup>1</sup>H–<sup>31</sup>P coupling constant of 921 Hz is detected. The axial methyl protons of (OEC)P(CH<sub>3</sub>)<sub>2</sub> appear as a doublet at  $\delta$  −6.23 with a <sup>1</sup>H–<sup>31</sup>P coupling constant of 17.4 Hz. The protons of the axially bound phenyl ligands on (OEC)P(C<sub>6</sub>H<sub>5</sub>)<sub>2</sub> are seen as three signals centered at  $\delta$  5.33 (*p*-H), 4.85 (*m*-H), and 0.39 (*o*-H), respectively. Phosphorus resonances with characteristic proton coupling located in the high-field region of the spectrum (between  $\delta$  −94 and −255) could also be observed for all compounds.

**UV–Visible Spectra.** The UV–visible spectral data of each examined corrole in CH<sub>2</sub>Cl<sub>2</sub> are given in the Experimental Section. The spectral data obtained in a solution of PhCN and 0.1 M TBAP are summarized in Table 2, while Figure 2 shows two representative spectra, one of (OEC)P(H)<sub>2</sub> and a second of [(OEC)P(CH<sub>3</sub>)<sub>2</sub>]<sup>+</sup>ClO<sub>4</sub><sup>−</sup>. On the basis of the Soret band shape and position, the examined derivatives can be divided into two groups. The first includes phosphorus corroles containing two identical covalently bound axial ligands, i.e., (OEC)P(H)<sub>2</sub> (Figure 2a), (OEC)P(C<sub>6</sub>H<sub>5</sub>)<sub>2</sub>, and (OEC)P(CH<sub>3</sub>)<sub>2</sub>. This group of complexes is characterized by a quite unusual split Soret band with two sharp maxima located between 425 and 446 nm. The second group of corroles is represented by (OEC)P=O and [(OEC)P(CH<sub>3</sub>)<sub>2</sub>]<sup>+</sup>ClO<sub>4</sub><sup>−</sup>. These two compounds exhibit *normal*

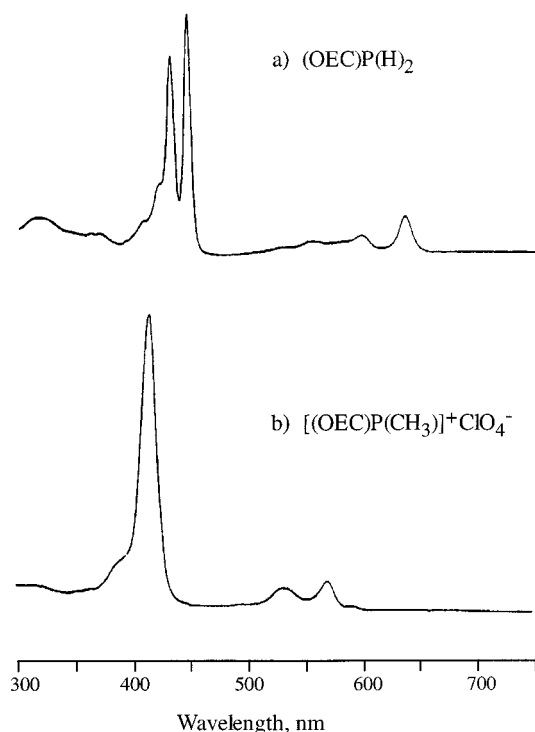


**Figure 2.** UV-visible spectra of (a) (OEC)P(H)<sub>2</sub> and (b) [(OEC)P(CH<sub>3</sub>)]<sup>+</sup>ClO<sub>4</sub><sup>-</sup> in PhCN.

**Table 3.** Half-Wave Potentials of Phosphorus Corroles (V vs SCE) in a Solution of PhCN and 0.1 M TBAP

compound	oxidation			reduction	
	3rd	2nd	1st	1st	2nd
(OEC)P=O	1.81 <sup>a</sup>	1.17 <sup>a</sup>	0.80	-1.58	
(OEC)P(H) <sub>2</sub>	1.81 <sup>a</sup>	1.10 <sup>a</sup>	0.44 <sup>a</sup>	-1.67	
(OEC)P(CH <sub>3</sub> ) <sub>2</sub>	1.79 <sup>a,b</sup>	1.12	0.44	-1.75	
(OEC)P(C <sub>6</sub> H <sub>5</sub> ) <sub>2</sub>	1.63 <sup>a</sup>	1.30 <sup>a</sup>	0.56	-1.71	
[(OEC)P(CH <sub>3</sub> )] <sup>+</sup> ClO <sub>4</sub> <sup>-</sup>	1.81 <sup>a</sup>	1.11 <sup>c</sup>	1.11 <sup>c</sup>	-1.16 <sup>d</sup>	-1.71

<sup>a</sup>  $E_{pa}$ , at scan rate of 100 mV/s. <sup>b</sup> A small peak can also be seen at  $E_{pa} = 1.46$  V. <sup>c</sup> The first two oxidations are overlapped in potential, giving directly a doubly oxidized P(V) corrole after the global abstraction of two electrons. <sup>d</sup>  $E_{pc}$ , at scan rate of 100 mV/s. A reversible reoxidation process can also be seen at  $E_{1/2} = 0.48$  V after the first reduction (see text for details).

UV-visible absorption spectra with a single Soret band as seen in Figure 2b for the case of [(OEC)P(CH<sub>3</sub>)]<sup>+</sup>ClO<sub>4</sub><sup>-</sup>.

**Electrochemistry of (OEC)P(CH<sub>3</sub>)<sub>2</sub> and (OEC)P(C<sub>6</sub>H<sub>5</sub>)<sub>2</sub>.** Redox potentials for the CH<sub>3</sub> and C<sub>6</sub>H<sub>5</sub> complexes are summarized in Table 3. Both corroles undergo a single reversible one-electron reduction located at  $E_{1/2} = -1.75$  V for (OEC)P(CH<sub>3</sub>)<sub>2</sub> and  $-1.71$  V for (OEC)P(C<sub>6</sub>H<sub>5</sub>)<sub>2</sub>. The first oxidation of both complexes is also reversible and occurs at 0.44 V for (OEC)P(CH<sub>3</sub>)<sub>2</sub> and at 0.56 V for (OEC)P(C<sub>6</sub>H<sub>5</sub>)<sub>2</sub> (see parts a and b of Figure 3, respectively). The one-electron chemical oxidation product of (OEC)P(CH<sub>3</sub>)<sub>2</sub> with 1 equiv of AgClO<sub>4</sub> exhibits a sharp isotropic ESR spectrum centered at  $g = 2.00$ , thus indicating formation of a phosphorus(V) corrole  $\pi$ -cation radical. Thin-layer UV-visible spectral changes, which are observed during the first one-electron oxidation and the first one-electron reduction of (OEC)P(CH<sub>3</sub>)<sub>2</sub>, are shown in Figure 4 and are in agreement with the formation of corrole  $\pi$ -cation and  $\pi$ -anion radicals after oxidation or reduction.

**Electrochemistry of (OEC)P=O and (OEC)P(H)<sub>2</sub>.** The oxo and dihydrido phosphorus(V) corroles undergo a single reversible one-electron reduction at  $E_{1/2} = -1.58$  V for (OEC)P=O

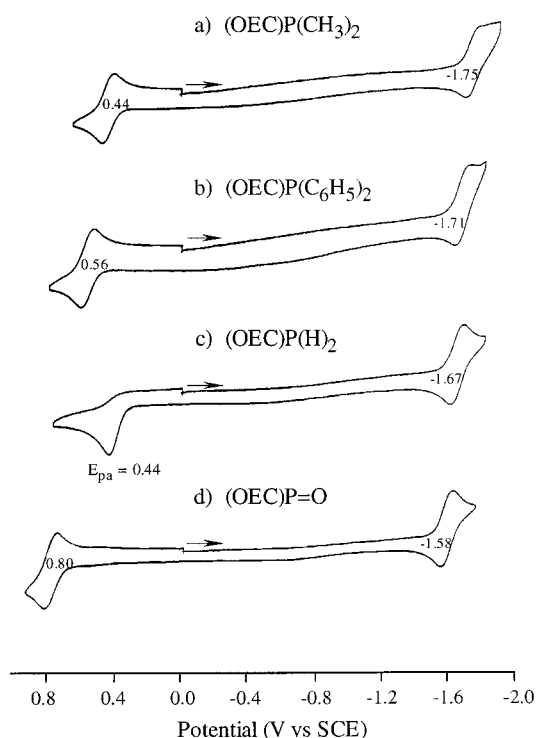


**Figure 3.** Cyclic voltammograms of (a) (OEC)P(CH<sub>3</sub>)<sub>2</sub>, (b) (OEC)P(C<sub>6</sub>H<sub>5</sub>)<sub>2</sub>, (c) (OEC)P(H)<sub>2</sub>, and (d) (OEC)P=O in a solution of PhCN and 0.1 M TBAP.

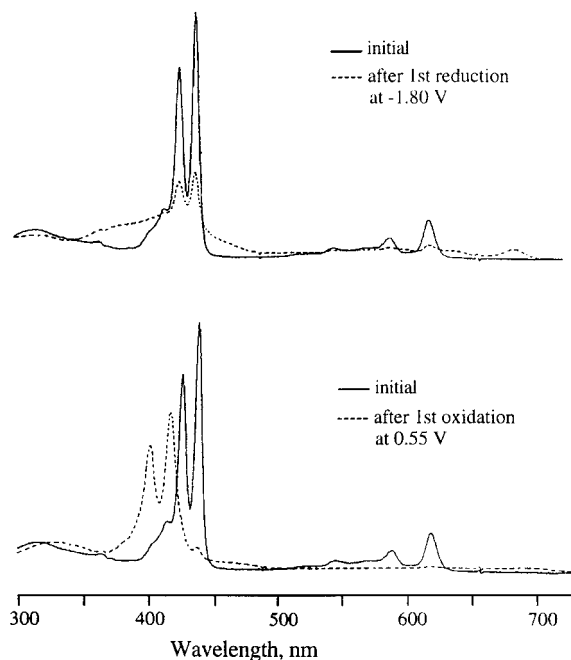


**Figure 4.** UV-visible spectral changes of (OEC)P(CH<sub>3</sub>)<sub>2</sub> in a solution of PhCN and 0.2 M TBAP before and after controlled-potential reduction (at  $-1.80$  V) and oxidation (at  $0.55$  V).

and  $-1.67$  V for (OEC)P(H)<sub>2</sub>, both of which are assigned as leading to phosphorus(V) corrole  $\pi$ -anion radicals based on UV-visible spectroelectrochemical data. The first oxidation of (OEC)P=O is reversible and located at  $E_{1/2} = 0.80$  V, while (OEC)P(H)<sub>2</sub> is irreversibly oxidized at  $E_{pa} = 0.44$  V (Figure 3c).

**Electrochemistry of [(OEC)P(CH<sub>3</sub>)]<sup>+</sup>ClO<sub>4</sub><sup>-</sup>.** Figure 5a shows cyclic voltammograms of [(OEC)P(CH<sub>3</sub>)]<sup>+</sup>ClO<sub>4</sub><sup>-</sup> in PhCN containing 0.1 M TBAP. The phosphorus(V) complex

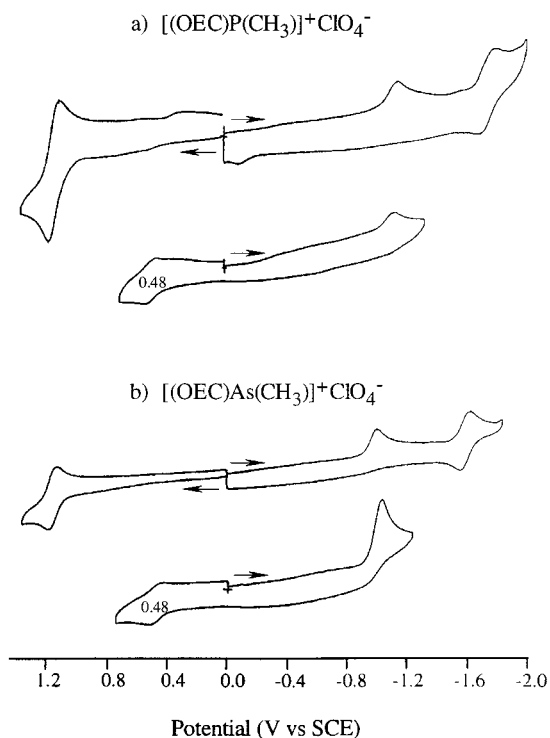


**Figure 5.** Cyclic voltammograms of (a)  $[(\text{OEC})\text{P}(\text{CH}_3)]^+\text{ClO}_4^-$  and (b)  $[(\text{OEC})\text{As}(\text{CH}_3)]^+\text{ClO}_4^-$  in a solution of PhCN and 0.1 M TBAP. The oxidation processes at 0.48 V are not seen upon initial positive potential scans and result, in both cases, from a product of the first reduction.

undergoes one reversible oxidation (at  $E_{1/2} = 1.11$  V) and two reductions, the first of which is irreversible and leads to formation of a product that can be reversibly oxidized at  $E_{1/2} = 0.48$  V (see Figure 5). The one-electron reduction of  $[(\text{OEC})\text{P}(\text{CH}_3)]^+\text{ClO}_4^-$  at  $E_{\text{pc}} = -1.16$  V leads to what is assigned as a P(III) product on the basis of comparisons with the electrochemistry of  $[(\text{OEC})\text{As}(\text{CH}_3)]^+\text{ClO}_4^-$  under the same experimental conditions.<sup>19</sup> The first oxidation of  $[(\text{OEC})\text{P}(\text{CH}_3)]^+\text{ClO}_4^-$  involves two overlapping one-electron-transfer steps at  $E_{1/2} = 1.11$  V and gives rise to an oxidation current that is double that for the first reduction at  $-1.16$  V. The two oxidation processes could not be resolved at room temperature in PhCN containing 0.1 M TBAP, but separate processes could be seen when the measurements were carried out at a lower temperature of 0 °C.

The electroreduction behavior of  $[(\text{OEC})\text{P}(\text{CH}_3)]^+\text{ClO}_4^-$  is almost identical to that of  $[(\text{OEC})\text{As}(\text{CH}_3)]^+\text{ClO}_4^-$  whose electrochemistry has been reported<sup>19</sup> and whose cyclic voltammograms are also shown in Figure 5. The voltammetric and spectroscopic data suggest the formation of a phosphorus(III) derivative upon the first reduction of  $[(\text{OEC})\text{P}(\text{CH}_3)]^+\text{ClO}_4^-$ , which is different from the product obtained after reduction of  $(\text{OEC})\text{P}(\text{H})_2$  or  $(\text{OEC})\text{P}=\text{O}$  at more negative half-wave potentials of  $-1.67$  or  $-1.58$  V, respectively. Thin-layer controlled-potential reduction of  $[(\text{OEC})\text{P}(\text{CH}_3)]^+\text{ClO}_4^-$  at  $-1.30$  V results in a disappearance of the band at 412 nm and the appearance of a new split Soret band (with maxima at 417 and 422 nm) and three to four bands in the visible region. We were unable to isolate this product, but the formation of a phosphorus(III) species is strongly suggested by electrochemical measurements made after bulk controlled-potential reduction at  $-1.30$  V in a solution of PhCN and 0.2 M TBAP. After bulk electrolysis, the reduction process of  $[(\text{OEC})\text{P}(\text{CH}_3)]^+\text{ClO}_4^-$  at  $E_{\text{pc}} = -1.16$

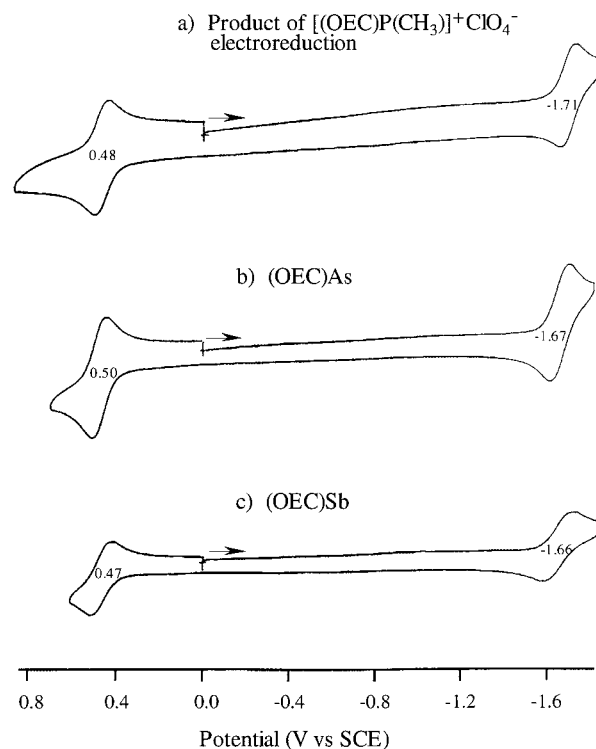


**Figure 6.** Cyclic voltammograms of (a)  $[(\text{OEC})\text{P}^{\text{V}}(\text{CH}_3)]^+\text{ClO}_4^-$  reduction product after bulk electrolysis at  $-1.30$  V in a solution of PhCN and 0.2 M TBAP and of (b)  $(\text{OEC})\text{As}^{\text{III}}$  and (c)  $(\text{OEC})\text{Sb}^{\text{III}}$  in a solution of PhCN and 0.1 M TBAP. The electrochemistry of the As(III) and Sb(III) complexes is discussed in ref 19.

V disappeared and the resulting cyclic voltammogram was virtually identical to that of  $(\text{OEC})\text{As}^{\text{III}}$  and  $(\text{OEC})\text{Sb}^{\text{III}}$  as seen in Figure 6.

**HOMO–LUMO Gap in Main Group Corroles.** It is well-known that the redox properties of a given metalloporphyrin will depend on the basicity of the macrocycle, the nature of the central metal ion, and the type of axial ligands.<sup>34,35</sup> We earlier reported the effects of substituents on the redox potentials of triphenylcorrolatocobalt(III) and showed a linear correlation to exist between the sum of the Hammett substituent constants on the macrocycle,  $\sum\sigma$ , and  $E_{1/2}$  for electrode processes at the metal or the macrocycle.<sup>36</sup> Linear relationships are often seen between  $E_{1/2}$  and  $\sum\sigma$  when very similar complexes with different electron-donating or electron-withdrawing substituents are examined (i.e., those containing the same central metal in the same oxidation state and with the same set of axial ligands). These types of correlations cannot be used for the main group corroles that contain four different central ions in two different oxidation states of +3 and +5 and five different axial ligand combinations because all of the compounds have the same OEC macrocycle, thus making the predictive use of Hammett parameters unsuitable for analysis of these compounds using this correlation.

To look for systematic trends in this particular group of metalcorroles, we have therefore utilized the Mulliken–Jaffé concept of electronegativity where the electronegativity of an atom in the molecule depends on the surrounding atoms or

(34) Kadish, K. M. *Prog. Inorg. Chem.* **1986**, *34*, 435.

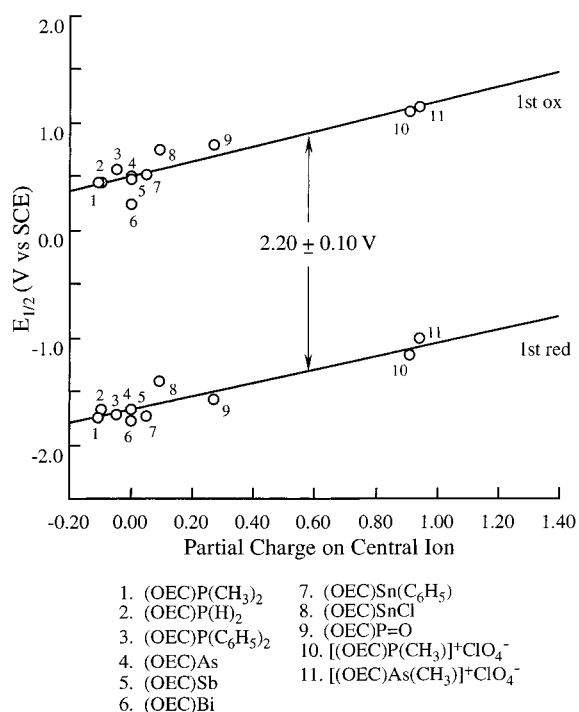
(35) Kadish, K. M.; Van Caemelbecke, E.; Royal, G. In *The Porphyrin Handbook*; Kadish, K. M., Smith, K. M., Guillard, R., Eds.; Academic Press: Burlington, MA, 2000; Vol. 8, pp 1–97.

(36) Adamian, V. A.; D'Souza, F.; Licocchia, S.; Di Vona, M. L.; Tassoni, E.; Paolesse, R.; Boschi, T.; Kadish, K. M. *Inorg. Chem.* **1995**, *34*, 532.

**Table 4.** Electronegativities ( $\chi$ ) and Partial Charge of Central Ion ( $\delta$ ) of Main Group Corroles along with Half-Wave Potentials for Their First Reduction and First Oxidation (V vs SCE) in a Solution of PhCN and 0.1 M TBAP

compound	$\chi^a$	$\delta^b$	first ox.	first red.	$\Delta E_{1/2}$
[(OEC)P(CH <sub>3</sub> ) <sub>2</sub> ] <sup>+</sup>	19.20	0.91	1.11	-1.16 <sup>d,e</sup>	2.27
(OEC)P=O	11.96	0.27	0.80	-1.58	2.38
(OEC)P(C <sub>6</sub> H <sub>5</sub> ) <sub>2</sub>	8.39	-0.05	0.56	-1.71	2.27
(OEC)P(H) <sub>2</sub>	7.80	-0.10	0.44 <sup>c</sup>	-1.67	2.11
(OEC)P(CH <sub>3</sub> ) <sub>2</sub>	7.70	-0.11	0.44	-1.75	2.19
[(OEC)As(CH <sub>3</sub> ) <sub>2</sub> ] <sup>+</sup>	16.75	0.94	1.16	-1.01 <sup>d,e</sup>	2.17
(OEC)As	8.30	0.0	0.50	-1.67	2.17
(OEC)Sb	8.48	0.0	0.47	-1.66	2.13
(OEC)Bi		0.0	0.24	-1.77	2.01
(OEC)SnCl	8.35	0.09	0.76	-1.41 <sup>d</sup>	2.16
(OEC)Sn(C <sub>6</sub> H <sub>5</sub> )	8.13	0.05	0.52	-1.73	2.25

<sup>a</sup> Electronegativity of central ion corrected for the effect of axial ligand(s) according to ref 37. <sup>b</sup> Partial charge of central ion. <sup>c</sup>  $E_{pa}$ , at scan rate of 100 mV/s. <sup>d</sup>  $E_{pc}$ , at scan rate of 100 mV/s. <sup>e</sup> A reversible reoxidation wave can be seen at  $E_{1/2} = 0.48$  V.

**Figure 7.** Plot of half-wave potentials for the first reduction and first oxidation of main group octaethylcorroles vs the partial charge of the central ion.

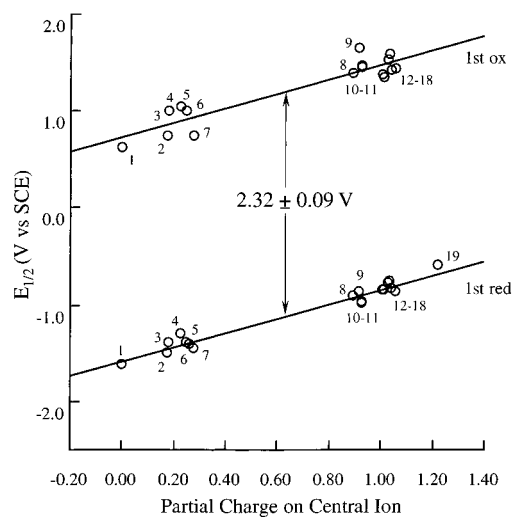
groups.<sup>37</sup> The electronegativity of the central ion in the case of the corroles,  $\chi_M$ , is affected by both the axial ligands and the total charge of the complex and can be calculated as shown in eqs 1 and 2, where  $a_M$ ,  $b_M$  and  $a_L$ ,  $b_L$  are the Mulliken–Jaffé coefficients for the central ion and the axial ligand, respectively,  $\delta$  is the partial charge on the central ion, and  $q$  is the ionic charge of the complex.

$$\chi_M = a_M + \delta b_M \quad (1)$$

$$\delta = \frac{a_L - a_M}{b_L + b_M} + q \quad (2)$$

The data of  $\chi$ ,  $\delta$ , and the HOMO–LUMO gap of the examined group of metalloporroles are summarized in Table 4.

(37) *Inorganic Chemistry, Principles of Structure and Reactivity*, 3rd ed.; Huheey, J. E., Ed.; Harper & Row: Publishers: New York, 1983.



- (OEP)Zn
- (OEP)Al(CH<sub>3</sub>)
- (OEP)GaCl
- (OEP)InCl
- (OEP)GaF
- (OEP)Si(OH)<sub>2</sub>
- (OEP)Al(C<sub>6</sub>H<sub>5</sub>)
- [(OEP)P(CH<sub>3</sub>)<sub>2</sub>]<sup>+</sup>
- [(OEP)Sb(CH<sub>3</sub>)<sub>2</sub>]<sup>+</sup>
- [(OEP)As(CH<sub>3</sub>)<sub>2</sub>]<sup>+</sup>
- [(OEP)As(CH<sub>3</sub>)(C<sub>2</sub>H<sub>5</sub>)<sub>2</sub>]<sup>+</sup>
- [(OEP)As(C<sub>2</sub>H<sub>5</sub>)<sub>2</sub>]<sup>+</sup>
- [(OEP)P(CH<sub>3</sub>)(OH)]<sup>+</sup>
- [(OEP)P(C<sub>2</sub>H<sub>5</sub>)(OH)]<sup>+</sup>
- [(OEP)P(CH<sub>3</sub>)(F)]<sup>+</sup>
- [(OEP)Sb(C<sub>2</sub>H<sub>5</sub>)(OH)]<sup>+</sup>
- [(OEP)P(C<sub>6</sub>H<sub>5</sub>)(OH)]<sup>+</sup>
- [(OEP)As(CH<sub>3</sub>)(OH)]<sup>+</sup>
- [(OEP)As(F)<sub>2</sub>]<sup>+</sup>

**Figure 8.** Plot of half-wave potentials for the first reduction and first oxidation of main group octaethylporphyrins vs the partial charge of the central ion.**Table 5.** Electronegativities ( $\chi$ ) and Partial Charge of Central Ion ( $\delta$ ) of Octaethylporphyrins along with Half-Wave Potentials<sup>a</sup> for Their First Reduction and First Oxidation (V vs SCE) in a Solution of CH<sub>2</sub>Cl<sub>2</sub> and 0.1 M TBAP

compound	$\chi^a$	$\delta^b$	first ox.	first red.	$\Delta E_{1/2}$
(OEP)Zn	4.71	0.00	0.63	-1.61	2.24
(OEP)Al(CH <sub>3</sub> )	6.63	0.17	0.75 <sup>c</sup>	-1.49	2.24
(OEP)GaCl	7.36	0.18	1.00	-1.38	2.38
(OEP)InCl	6.82	0.23	1.05	-1.29	2.34
(OEP)GaF	7.88	0.25	1.00	-1.38	2.38
(OEP)Si(OH) <sub>2</sub>	9.65	0.26		-1.40	
(OEP)Al(C <sub>6</sub> H <sub>5</sub> )	7.32	0.28	0.75 <sup>c</sup>	-1.44	2.19
[(OEP)P(CH <sub>3</sub> ) <sub>2</sub> ] <sup>+</sup>	19.03	0.89	1.39	-0.90	2.29
[(OEP)Sb(CH <sub>3</sub> ) <sub>2</sub> ] <sup>+</sup>	17.02	0.91	1.66 <sup>c</sup>	-0.86	2.52
[(OEP)As(CH <sub>3</sub> ) <sub>2</sub> ] <sup>+</sup>	16.62	0.92	1.45	-0.96	2.41
[(OEP)As(CH <sub>3</sub> )(C <sub>2</sub> H <sub>5</sub> ) <sub>2</sub> ] <sup>+</sup>	16.63	0.93	1.45	-0.96	2.41
[(OEP)As(C <sub>2</sub> H <sub>5</sub> ) <sub>2</sub> ] <sup>+</sup>	16.64	0.93	1.47	-0.97	2.44
[(OEP)P(CH <sub>3</sub> )(OH)] <sup>+</sup>	20.31	1.01	1.38	-0.84	2.22
[(OEP)P(C <sub>2</sub> H <sub>5</sub> )(OH)] <sup>+</sup>	20.32	1.01	1.35	-0.84	2.19
[(OEP)P(CH <sub>3</sub> )(F)] <sup>+</sup>	20.56	1.03	1.54	-0.77 <sup>d</sup>	2.31
[(OEP)Sb(C <sub>2</sub> H <sub>5</sub> )(OH)] <sup>+</sup>	18.15	1.03	1.60 <sup>c</sup>	-0.74	2.34
[(OEP)P(C <sub>6</sub> H <sub>5</sub> )(OH)] <sup>+</sup>	20.63	1.04	1.43	-0.82	2.25
[(OEP)As(CH <sub>3</sub> )(OH)] <sup>+</sup>	17.54	1.03	1.44	-0.86	2.30
[(OEP)As(F) <sub>2</sub> ] <sup>+</sup>	19.26	1.22		-0.58 <sup>d</sup>	

<sup>a</sup> Electronegativity of central ion corrected for the effect of axial ligand(s) according to refs 37 and 38. <sup>b</sup> Partial charge of central ion. <sup>c</sup>  $E_{pa}$ , at scan rate of 100 mV/s. <sup>d</sup>  $E_{pc}$ , at scan rate of 100 mV/s. <sup>e</sup> Redox potentials taken from ref 40.

The half-wave potentials correlate well with the Mulliken–Jaffé electronegativity or the partial charge of the central ions corrected for the inductive effect of the axial ligand<sup>37,38</sup> and the ionic charge of the complex. A correlation between  $E_{1/2}$  and the partial charge on the central ion is shown in Figure 7. One can see from this figure that an increase in partial charge on the main group ion results in an easier first reduction and a harder first oxidation of the complex. This general trend is also seen in Figure 8 for a similar series of complexes containing octaethylporphyrin (OEP) macrocycles.

(38) Huheey, J. E. *J. Phys. Chem.* **1965**, *69*, 3284.

The electrochemical HOMO–LUMO gap of metalloporphyrins has often been used as a diagnostic criterion for assigning the site of electron transfer to the metal or the macrocycle. The value of the HOMO–LUMO gap has been given as  $2.25 \pm 0.15$  V for reactions at the conjugated  $\pi$ -ring system of metalloporphyrins containing OEP or tetraphenylporphyrin (TPP) macrocycles<sup>34,35</sup> (see Figure 8 and Table 5), and a very similar value of  $2.20 \pm 0.10$  V is seen for the main group metalloporphyrins in Figure 7 for reactions involving either the ring or the central ion.

---

(39) D'Souza, F.; Boulas, P.; Aukauloo, A. M.; Guillard, R.; Kisters, M.; Vogel, E.; Kadish, K. M. *J. Phys. Chem.* **1994**, *98*, 11885.

(40) Kadish, K. M.; Royal, G.; Van Caemelbecke, E.; Gueletti, L. In *The Porphyrin Handbook*; Kadish, K. M., Smith, K. M., Guillard, R., Eds.; Academic Press: Burlington, MA, 2000; Vol. 9, pp 1–114.

The excellent linear correlation in Figure 7 is somewhat surprising because the potentials include both ring-centered and metal-centered processes of the corroles. Metal-centered processes of metalloporphyrins have not generally been thought to fit correlations with ring-centered processes.<sup>35,39</sup> The data in Figure 7 therefore imply that the actual site of the electron transfer in the examined group of complexes does not determine the half-wave potentials that are related to the overall charge of the complex and the nature of the central ion, i.e., the HOMO and LUMO orbitals in the main group corroles may involve both orbitals of the macrocycle and those of the central ion.

**Acknowledgment.** The support of the Robert A. Welch Foundation (K.M.K., Grant E-680) is gratefully acknowledged.

IC0010196